

Grid Integration of Distributed Wind Generation: Hybrid Markovian and Interval Unit Commitment

Yaowen Yu, *Student Member, IEEE*, Peter B. Luh, *Fellow, IEEE*, Eugene Litvinov, *Fellow, IEEE*,
Tongxin Zheng, *Senior Member, IEEE*, Jinye Zhao, *Member, IEEE*, and Feng Zhao, *Member, IEEE*

Abstract—Grid integration of wind generation is challenging in view of wind uncertainties and possible transmission congestions. Without considering transmission, a stochastic unit commitment problem was solved in our previous work by modeling aggregated wind as a Markov chain instead of scenarios for reduced complexity. With congestion, wind generation at different locations cannot be aggregated and is modeled as a Markov chain per wind node, and the resulting global states are a large number of combinations of nodal states. To avoid explicitly considering all such global states, interval optimization is synergistically integrated with the Markovian approach in this paper. The key is to divide the generation level of a conventional unit into a Markovian component that depends on the local state, and an interval component that manages extreme nonlocal states. With appropriate transformations, the problem is converted to a linear form and is solved by using branch-and-cut. Numerical results demonstrate that the over conservativeness of pure interval optimization is much alleviated, and the new approach is effective in terms of computational efficiency, simulation cost, and solution feasibility. In addition, solar generation shares a similar uncertain nature as wind generation, and can thus be modeled and solved similarly.

Index Terms—Interval optimization, Markov decision process, unit commitment (UC), wind generation.

I. INTRODUCTION

WIND ENERGY can help to reduce the dependence on fossil fuels and greenhouse gas emissions, and the global wind industry has been growing rapidly. In 2012, nearly 45 GM of wind capacity was brought online, and the global wind capacity was increased by 19% to almost 283 GW [2]. The U.S. Department of Energy sets the target to increase wind energy's contribution to 20% of electricity by 2030 [3].

Manuscript received July 8, 2014; revised March 5, 2015; accepted May 4, 2015. This work was supported in part by the National Science Foundation under Grant ECCS-1028870, and in part by the Project through ISO New England. A preliminary and abridged version [1] was presented in the 2012 IEEE Power and Energy Society General Meeting, San Diego, CA, USA, July 2012. Any opinions, findings, and conclusions or recommendations expressed in this paper are those of the authors and do not necessarily reflect the views of the National Science Foundation. Paper no. TSG-00698-2014.

Y. Yu and P. B. Luh are with the Department of Electrical and Computer Engineering, University of Connecticut, Storrs, CT 06269 USA (e-mail: yaowen.yu@engr.uconn.edu).

E. Litvinov, T. Zheng, J. Zhao, and F. Zhao are with the Business Architecture and Technology Department, ISO New England, Holyoke, MA 01040 USA.

Color versions of one or more of the figures in this paper are available online at <http://ieeexplore.ieee.org>.

Digital Object Identifier 10.1109/TSG.2015.2430851

Wind integration involves wind turbine technologies, power electronics, power systems, and market design issues. Related fundamentals of power systems include long-term planning, improved forecasting, operational processes and tools, and smart grid technologies [4].

A critical operational process is day-ahead unit commitment (UC) in which the independent system operator (ISO) commits conventional units to meet the forecasted demand of the following day while satisfying individual unit and transmission constraints. UC with high levels of wind generation, however, is challenging in light of the fact that wind generation is uncertain by nature and transmission congestions are possible. A straight-forward way to address uncertainty in this process is the deterministic approach that meets the expected system demand and adjusts reserve levels based on hourly standard deviations (STDs) of wind generation [5], [6]. Since wind uncertainties are not explicitly captured, solutions may be infeasible for certain wind generation realizations [7].

Besides the deterministic approach, several other approaches have been presented in the literature, including stochastic programming, robust optimization, and interval optimization. Stochastic programming optimizes the expected cost over the probability distribution of uncertainties, with wind uncertainties commonly modeled by representative scenarios [8]–[15]. A scenario contains a trajectory of realizations over all hours in the time horizon, and the number of scenarios increases exponentially with the number of hours. It is difficult to select an appropriate number of scenarios to balance modeling accuracy, solution feasibility, and computational efficiency. Robust optimization finds the optimal solution of the worst-case realization in a given uncertainty set to ensure solution feasibility against all possible realizations, and may lead to conservative solutions [7], [16], [17]. In addition, the two-stage robust model in [7] is nonlinear and computationally challenging. Interval optimization is another approach for linear problems with uncertainties modeled by intervals [14], [18]. The approach captures bounds of uncertain wind generation in system demand and transmission capacity constraints. Other realizations within these bounds will be guaranteed to be feasible. The effective use of interval arithmetic makes this approach computationally efficient. However, its results remain conservative. The literature is reviewed in Section II.

To overcome the difficulties of existing approaches, a pure Markovian approach was developed in our previous work to

solve the day-ahead stochastic UC problem without transmission constraints [19]. Wind generation from all wind farms was aggregated and modeled as a Markov chain with state transition matrices established based on historical data. The UC problem was then formulated as a stochastic optimization problem based on states instead of scenarios. A state represents the wind generation value at a particular hour and captures past information probabilistically. Because the number of states increases linearly with the number of hours, the complexity of the problem is significantly reduced when compared to scenario-based formulations. With state transitions linearly formulated, the problem was effectively solved by using the branch-and-cut method [20], [21].

In this paper, the pure Markovian approach in [19] is extended to consider transmission constraints. Since possible congestions imply that wind generation at different locations needs to be treated separately, wind generation is modeled as a Markov chain for each wind node.¹ There are multiple Markov chains in a transmission network. These chains are assumed independent for simplicity. The resulting global states are a large number of combinations of local/nodal states. Dispatch decisions of pure Markov-based optimization [19] should explicitly depend on the global states. To reduce this complexity, an approach that synergistically incorporates both Markov-based optimization and interval optimization is developed. The new hybrid Markovian and interval approach has the following three main contributions.

- 1) To make use of information from local states without considering all possible global states, the generation level (dispatch decision) of a conventional unit is divided into two components: the Markovian component that depends on the local state and the interval component that manages extreme nonlocal states.
- 2) Constraints are innovatively formulated to guarantee solution feasibility for all possible realizations without much complexity. Especially, the effective use of local wind states alleviates the over conservativeness of interval optimization in transmission capacity and ramp rate constraints.
- 3) By analyzing the monotonicity of Markovian nodal injections, the problem is transformed into a linear form and is efficiently solved by using branch-and-cut.

Section III models distributed wind generation, presents pure Markov-based optimization, formulates the new hybrid Markovian and interval approach, and discusses two methods to reduce the wind uncertainty by considering wind power forecasts or incorporating spatial correlations of wind farms. Section IV develops the solution methodology, and compares the complexity and conservativeness of the new approach with those of pure Markov-based optimization and pure interval optimization. Section V tests a simple problem, the IEEE 30-bus system, and the IEEE 118-bus system. Numerical results demonstrate that our approach alleviates the over conservativeness of interval optimization and is effective

in terms of computational efficiency, simulation cost, and solution feasibility.

Although the problem solved in this paper is day-ahead UC, the new formulation is general and can model real-time UC as well. In addition, solar generation can be modeled and solved in ways similar to those for wind generation. The reason is that even though wind and solar have different diurnal patterns—peak wind generation usually occurs in the morning and evening while that of solar usually occurs in the middle of a day [23], they share the similar uncertain nature.

II. LITERATURE REVIEW

This section reviews stochastic programming, robust optimization, pure interval optimization, and hybrid approaches.

A. Stochastic Programming

It optimizes the expected cost over the probability distribution of uncertainties, with wind uncertainties commonly modeled by using representative scenarios [8]–[15]. A single set of UC decisions are determined to satisfy all the selected scenarios, together with multiple sets of dispatch decisions, one for each scenario. The objective is to minimize the commitment cost and the expected dispatch cost. Decomposition methods, such as Benders' decomposition [9], [14] or Lagrangian relaxation [13], [15], are used to solve stochastic UC problems.

Typically, wind generation or wind speed at each hour is assumed to follow a distribution to generate scenarios. Each scenario represents a sequence of realizations of uncertainties over the optimization horizon (e.g., 24 h). As a result, the number of scenarios can be extremely large even when dealing with discrete probability distributions. Therefore, scenario reduction techniques are commonly used to eliminate very low-probability scenarios, to aggregate “close” scenarios [24], [25], or to measure the impact of each scenario on the objective function [26]. The reduced number of scenarios is then considered in the stochastic UC problem. In general, it is difficult to select an appropriate number of scenarios to balance modeling accuracy, solution feasibility, and computational efficiency. To refine the number of scenarios while retaining high-impact rare events, 11 criteria (e.g., the minimum possible wind output throughout the day) are discussed to select scenarios [13]. These criteria, however, are heuristic in nature based on daily patterns of wind, so important rare events of abnormal days may not be captured. Additionally, it is not clear how to extend this method to networks with multiarea wind production and transmission constraints [15]. The alternative selection method presented in [15] ignores rare events with questionable validity.

B. Robust Optimization

It seeks an optimal solution feasible for all possible realizations within a predetermined uncertainty set. With uncertainties modeled by the uncertainty set without probabilistic information, it optimizes against the worst-case realization to ensure feasibility of all possible realizations [7], [16], [17]. The worst-case design avoids the combinatorial complexity

¹The Markovian model was validated in [22] for day-ahead and real-time wind generation series.

caused by nodal uncertainties when all possible realizations are considered. The robust UC model in [7] has two stages. The first stage is to determine the optimal UC decisions feasible for all possible realizations by using Benders decomposition; and the second is to select dispatch decisions against the worst-case realization given in UC decisions of the first stage by using outer approximation. Numerical experiments demonstrate that this approach is insensitive to different underlying probability distributions of wind generation. However, optimization of the worst-case realization leads to a conservative solution, which is a common concern of the robust optimization approach. In addition, the two-stage robust model in [7] is nonlinear and computationally challenging.

C. Pure Interval Optimization

It is another approach for linear problems with uncertainties modeled by closed intervals [14], [18]. Interval arithmetic captures bounds of uncertain wind generation in system demand and transmission capacity constraints, and a set of UC decisions are required to be feasible for all these bounds [18].

Wind generation for node i at hour t is denoted as $\tilde{p}_i^W(t)$ (MW), and is assumed to be within an interval $[p_i^W(t), \bar{p}_i^W(t)]$. System demand constraints require that total wind generation plus total conventional generation equal system demand for each hour. Based on [18, eq. (20)], the lower bound of total wind generation happens at the minimum realization m (when the outputs of all wind farms are at their lower limits), while the upper bound occurs at the maximum realization M . UC decisions of conventional units are required to meet these bounds in system demand constraints, so that any other realizations within these bounds will be satisfied. For example, two wind farms are in a transmission network. Wind farm 1 can generate from 10 to 40 MW, wind farm 2 can generate from 20 to 50 MW, and system demand is 200 MW. The total wind generation is from 30 to 90 MW, and the resulting net system demand (= system demand – wind generation) is from 110 to 170 MW. If a set of UC decisions can meet the minimum net system demand at 110 MW and the maximum net system demand at 170 MW, then it will be able to meet any net system demand within them. Such minimum and maximum system demand constraints are

$$\sum_i \sum_k p_{i,k,m}(t) = \sum_i p_i^L(t) - \sum_i p_i^W(t), \quad \forall t \quad (1)$$

$$\sum_i \sum_k p_{i,k,M}(t) = \sum_i p_i^L(t) - \sum_i \bar{p}_i^W(t), \quad \forall t \quad (2)$$

where $p_{i,k,m}(t)$ is the dispatch decision of conventional unit k at node i (or unit i,k) at time t under the minimum wind realization, $p_{i,k,M}(t)$ under the maximum wind realization, and $p_i^L(t)$ is the demand at node i at time t .

Transmission capacity constraints imply that the power flow through line l at time t , denoted as $f_l(t)$, cannot exceed its transmission capacity f_l^{\max} , that is

$$-f_l^{\max} \leq f_l(t) \leq f_l^{\max}, \quad \forall l, \forall t. \quad (3)$$

In dc power flow, a line flow is a linear combination of nodal injections weighted by generation shift factors (GSFs).

When the dispatch decision of unit i,k is $p_{i,k}(t)$, the power flow is

$$f_l(t) = \sum_i a_l^i \left(\sum_k p_{i,k}(t) + \tilde{p}_i^W(t) - p_i^L(t) \right), \quad \forall l, \forall t \quad (4)$$

where a_l^i is the GSF representing the sensitivity of $f_l(t)$ with respect to the nodal injection (= nodal generation – nodal demand) from node i . Similar to system demand constraints (1) and (2), the bounds of wind uncertainties through each line are captured based on [18, eqs. (16) and (19)]

$$\begin{aligned} & \sum_i \left(a_l^i \sum_k p_{i,k}(t) \right) \\ & \geq -f_l^{\max} - \min \left[\sum_i a_l^i (\tilde{p}_i^W(t) - p_i^L(t)) \right], \quad \forall l, \forall t \quad (5) \end{aligned}$$

$$\begin{aligned} & \sum_i \left(a_l^i \sum_k p_{i,k}(t) \right) \\ & \leq f_l^{\max} - \max \left[\sum_i a_l^i (\tilde{p}_i^W(t) - p_i^L(t)) \right], \quad \forall l, \forall t. \quad (6) \end{aligned}$$

A difference is that GSFs can be positive or negative. Nevertheless, since only inputs are contained on the right-hand sides of (5) and (6), interval arithmetic can be used to compute these bounds before optimization. As long as one feasible solution can be found within bounds, all transmission capacity constraints through line l at time t will be feasible. Since system demand constraints have to be satisfied at the same time, two sets of dispatch decisions $\{p_{i,k,m}(t)\}$ and $\{p_{i,k,M}(t)\}$ are considered in (5) and (6).

Ramp rate constraints imply the change of generation level cannot exceed the unit's ramp rate between two consecutive hours. These constraints [18, eqs. (21) and (22)] are required to be feasible for the transitions of wind outputs between any pairs among the minimum, maximum, and the expected realization that is considered in the objective function. The objective function in [27] uses the cost of the worst-case realization as that considered in robust optimization. The resulting optimization solutions may be conservative. Alternatively, the expected cost of all realizations could be considered. Due to the lack of probabilistic information, the cost of the expected realization is considered for simplicity as the objective function in [18, eq. (1)]. In this case, the impacts of extreme realizations are not explicitly captured. The effective use of interval arithmetic makes this approach computationally efficient. However, results are still conservative. For the rest of this paper, pure interval optimization refers to that in [18].

In addition to the approaches reviewed above, there are also hybrid stochastic and robust/interval approaches. A hybrid stochastic and robust approach [28] considers dispatch decisions and constraints from both stochastic programming and robust optimization at the same time, and the objective function is a weighted sum of the costs from both approaches. This approach provides more robust UC decisions than stochastic programming and a lower simulation cost than robust optimization. Its robust optimization part remains nonlinear.

A hybrid stochastic/interval approach [29] considers decision variables, constraints and the cost from stochastic programming at the first few hours, and then switch to pure interval optimization at the remaining hours. This approach provides a lower simulation cost than stochastic programming or pure interval optimization. Its pure interval optimization part remains conservative.

III. PROBLEM FORMULATION

Section III-A models distributed wind generation as a Markov chain per wind node, and describes the UC problem. Section III-B presents pure Markov-based optimization with a few main formulas, and discusses its complexity. To reduce this complexity, Section III-C formulates the new hybrid Markovian and interval approach. Section III-D discusses two methods to reduce the wind uncertainty by considering wind power forecasts or by incorporating spatial correlations of wind farms.

A. Wind Model and the UC Problem

1) *Markovian Model of Nodal Wind Generation and Global State*: When transmission constraints are considered, wind generation at different locations cannot be aggregated and must be treated separately. For simplicity, wind generation at different network nodes is assumed to be modeled as independent Markov chains. Let i denotes a node in the network with I being the total number of nodes. Based on [19], wind generation at node i is discretized into N_i states. These states are arranged in the ascending order of wind generation values. The transition probability from state n'_i to n_i is based on historical data

$$\pi_{n'_i n_i} = \frac{\text{observed transitions from state } n'_i \text{ to } n_i}{\text{occurrences of state } n'_i}. \quad (7)$$

Denote wind generation of state n_i at time t as $p_{i,n_i}^W(t)$ (MW). Its probability, denoted as $\varphi_{n_i}(t)$, can be computed by using probabilities of previous states and transition probabilities

$$\varphi_{n_i}(t) = \sum_{n'_i=1}^{N_i} \pi_{n'_i n_i} \varphi_{n'_i}(t-1). \quad (8)$$

A global state at time t , denoted as g , is a combination of wind generation states at all nodes, that is

$$g \equiv [n_1, n_2, \dots, n_I]^T. \quad (9)$$

Its probability at time t is denoted as $\varphi_g(t)$ and can be computed as the product of probabilities of all nodal states. Given that each node has up to N possible states at time t , the number of possible global states can be N^I , which is extremely large for practical problems.

2) *UC Problem Setup*: Building on [19] and [30], let K_i units at node i be indexed by (i, k) ($1 \leq k \leq K_i$) and L transmission lines be indexed by l ($1 \leq l \leq L$) in a day-ahead energy market over 24 (T) hours indexed by t ($1 \leq t \leq T$). Unit k at node i has an increasing convex piecewise linear generation cost function $C_{i,k}(p_{i,k}(t))$ (\$) for multiple generation blocks, a start-up cost $S_{i,k}$ (\$/Start), a no-load cost $S_{i,k}^{NL}$ (\$),

minimum and maximum generation levels $p_{i,k}^{\min}$ (MW) and $p_{i,k}^{\max}$ (MW), respectively, a ramp rate $R_{i,k}$ (MW/h), and minimum up and down times (h). The demand is assumed to be given and is denoted by $p_i^L(t)$ (MW) for node i at hour t . Line l has a transmission capacity f_l^{\max} (MW). The stochastic UC problem is to minimize the total cost by selecting a single set of UC decisions and multiple sets of dispatch decisions of conventional generators over a 24-h horizon. For the conventional unit i,k , the UC decision at time t is denoted by the binary variable $x_{i,k}(t)$, with “1” representing online and “0” offline. The start-up decision is denoted by the binary decision variable $u_{i,k}(t)$, with 1 representing start-up and 0 otherwise. Different sets of dispatch decisions will be made in pure Markov-based optimization to be presented in Section III-B and in the hybrid Markovian and interval approach in Section III-C.

B. Pure Markov-Based Optimization and Its Complexity

Dispatch decisions of the pure Markovian approach [19], denoted as $p_{i,k,g}(t)$ for unit i,k at time t at global state g , explicitly depend on the global states. The objective is to minimize the commitment cost plus the expected dispatch cost, that is

$$\min \sum_{t=1}^T \sum_{i=1}^I \sum_{k=1}^{K_i} \left\{ \sum_{g=m}^M [\varphi_g(t) C_{i,k}(p_{i,k,g}(t))] + u_{i,k}(t) S_{i,k} + x_{i,k}(t) S_{i,k}^{NL} \right\} \quad (10)$$

where m represents the minimum global state where all wind farms are at their minimum possible state, and M the maximum global state. System demand constraints (11) and transmission capacity constraints (12) are satisfied for all possible global states

$$\sum_i \sum_k p_{i,k,g}(t) + \sum_i p_{i,g}^W(t) = \sum_i p_{i,g}^L(t), \quad \forall t, \forall g \quad (11)$$

$$-f_l^{\max} \leq f_{l,g}(t) \leq f_l^{\max}, \quad \forall l, \forall t, \forall g. \quad (12)$$

In the above equation, $f_{l,g}(t)$ denotes the power flow though line l at time t at global state g and is represented based on GSFs as

$$f_{l,g}(t) = \sum_i \left[a_i^l \cdot \left(\sum_k p_{i,k,g}(t) + p_{i,g}^W(t) - p_{i,g}^L(t) \right) \right], \quad \forall l, \forall t, \forall g. \quad (13)$$

Individual unit constraints related to dispatch decisions include generator capacity constraints and ramp rate constraints. Generator capacity constraints are satisfied for possible global states. Ramp rate constraints are satisfied for possible state transitions from hour $t-1$ to t , that is

$$p_{i,k,g'}(t-1) - R_{i,k} \leq p_{i,k,g}(t) \leq p_{i,k,g'}(t-1) + R_{i,k} \\ \forall (g', g) \in \{(g', g) | \varphi_{g'}(t) > 0, \pi_{g'g} > 0\} \quad (14)$$

where g' denotes the global state at hour $t-1$. Since its dispatch decisions explicitly depend on a large number of possible global states, the pure Markov-based approach is very complex and thus not practical.

C. Hybrid Markovian and Interval UC Formulation

To reduce the dimension of the pure Markov-based stochastic UC problem, a synergistic combination of Markov-based optimization and interval optimization is developed.

1) *Local and Nonlocal States and Dispatch Decisions*: To avoid making dispatch decisions explicitly dependent on all possible realizations, our key idea is to divide the generation level (dispatch decision) of conventional unit $_{i,k}$ at time t into two components: $p_{i,k,n_i}^M(t)$ denotes the Markovian generation depending on local wind state n_i , and $p_{i,k,\bar{n}_i}^I(t)$ denotes the interval generation depending on extreme nonlocal states \bar{n}_i . For node i , its local state is the nodal wind state n_i . Its minimum possible local state is represented as $\min n_i$, and its maximum as $\max n_i$. Note that, $\min n_i$ may not be 1 at time t , since state 1 at node i may have zero probability. Its extreme nonlocal states \bar{n}_i are the minimum nonlocal state m_i and the maximum nonlocal state M_i , i.e., $\bar{n}_i \in \{m_i, M_i\}$. The minimum nonlocal state is a combination of possible minimum states of other nodes, that is

$$m_i \equiv [\min n_1, \dots, \min n_{i-1}, \min n_{i+1}, \dots, \min n_I]^T. \quad (15)$$

The maximum nonlocal state M_i is a combination of maximum possible states of other nodes, that is

$$M_i \equiv [\max n_1, \dots, \max n_{i-1}, \max n_{i+1}, \dots, \max n_I]^T. \quad (16)$$

In simulation, where only one global state is realized at an hour in each scenario, one level of conventional generation will be obtained. This generation level will be within the ranges delineated by sums of corresponding Markovian generation and interval generation levels.

In addition, the dispatch decisions corresponding to the expected realization E (where all wind farms are at their expected outputs), denoted as $p_{i,k,E}(t)$, will also be considered in the objective function to be discussed later. The constraints for the expected realization can be easily included as one set of deterministic constraints with the same set of commitment decisions $\{x_{i,k}(t)\}$ and one set of dispatch decisions $\{p_{i,k,E}(t)\}$. These constraints are not presented for conciseness. Constraints corresponding to the Markovian and interval dispatch decisions are formulated as follows.

2) *Nodal Level Analysis*: As a result of dividing the generation level, each nodal or unit-level constraint considers these two components. In particular, we have the following.

a) *Generator capacity constraints*: If the unit is committed, its generation level is within the minimum and maximum values; otherwise, its generation level should be zero

$$\begin{aligned} x_{i,k}(t) p_{i,k}^{\min} &\leq p_{i,k,n_i}^M(t) + p_{i,k,\bar{n}_i}^I(t) \\ &\leq x_{i,k}(t) p_{i,k}^{\max} \quad \forall i, \forall k, \forall t, \forall n_i \in \Omega_i(t), \forall \bar{n}_i \end{aligned} \quad (17)$$

where $\Omega_i(t)$ is the set of possible wind states at node i at hour t ($\Omega_i(t) \equiv \{n_i | \varphi_{n_i}(t) > 0\}$). For the rest of this paper, the expression, $n_i \in \Omega_i(t)$, is omitted.

b) *Nodal injections*: The nodal injection at node i is wind generation plus conventional generation minus demand, that is

$$\begin{aligned} P_{i,n_i,\bar{n}_i}(t) &= p_{i,n_i}^W(t) + \sum_k (p_{i,k,n_i}^M(t) + p_{i,k,\bar{n}_i}^I(t)) \\ &\quad - p_i^L(t), \quad \forall i, \forall t, \forall n_i, \forall \bar{n}_i. \end{aligned} \quad (18)$$

3) *System Demand Constraints*: Based on (1) and (2) [18, eq. (20)] as reviewed in the pure interval optimization part of Section II, as long as the minimum and maximum global states are satisfied, all other realizations will satisfy system demand at time t . In the minimum global state m , we have

$$\begin{aligned} \sum_i \sum_k p_{i,k,m_i}^I(t) \\ = \sum_i \left(p_i^L(t) - p_{i,\min n_i}^W - \sum_k p_{i,k,\min n_i}^M(t) \right), \quad \forall t. \end{aligned} \quad (19)$$

Similarly, system demand constraints at the maximum global state M are

$$\begin{aligned} \sum_i \sum_k p_{i,k,M_i}^I(t) \\ = \sum_i \left(p_i^L(t) - p_{i,\max n_i}^W - \sum_k p_{i,k,\max n_i}^M(t) \right), \quad \forall t. \end{aligned} \quad (20)$$

4) *Transmission Capacity Constraints*: DC power flow is used since it is sufficient for the UC purpose, and a line flow is a linear combination of nodal injections weighted by GSFs. Since GSFs can be positive or negative, the selection of extreme flow levels is more complicated than system demand. Therefore, the terms in the nodal injection in (18) are regrouped to a Markovian nodal injection consisting of those related to local states

$$P_{i,n_i}^M(t) \equiv p_{i,n_i}^W(t) + \sum_k p_{i,k,n_i}^M(t) - p_i^L(t), \quad \forall i, \forall t, \forall n_i \quad (21)$$

and an interval nodal injection related to nonlocal states

$$P_{i,\bar{n}_i}^I(t) \equiv \sum_k p_{i,k,\bar{n}_i}^I(t), \quad \forall i, \forall t, \forall \bar{n}_i. \quad (22)$$

For line l at time t , the flow has two parts corresponding to the two components of nodal injections from (21) and (22).

Wind uncertainties are contained in Markovian nodal injections, and bounds of Markovian flow levels are selected based on signs of GSFs and corresponding extreme Markovian nodal injections, that is

$$\begin{aligned} \sum_{i:a_l^i > 0} \left[a_l^i \cdot \min_{n_i} P_{i,n_i}^M(t) \right] + \sum_{i:a_l^i < 0} \left[a_l^i \cdot \max_{n_i} P_{i,n_i}^M(t) \right] \\ \leq f_{l,n_1,\dots,n_I}^M(t) = \sum_i \left[a_l^i \cdot P_{i,n_i}^M(t) \right] \\ \leq \sum_{i:a_l^i > 0} \left[a_l^i \cdot \max_{n_i} P_{i,n_i}^M(t) \right] \\ + \sum_{i:a_l^i < 0} \left[a_l^i \cdot \min_{n_i} P_{i,n_i}^M(t) \right], \quad \forall l, \forall t. \end{aligned} \quad (23)$$

The min/max operations to select extreme Markovian nodal injections are nonlinear and will be transformed to linear forms in Section IV-A.

The two sets of interval nodal injections from (19) and (20) can be directly translated to two interval flow levels, that is

$$f_{l,m}^l(t) = \sum_i [a_l^i \cdot P_{i,m_i}^l(t)], \quad \forall l, \forall t \quad (24)$$

$$f_{l,M}^l(t) = \sum_i [a_l^i \cdot P_{i,M_i}^l(t)], \quad \forall l, \forall t. \quad (25)$$

These two interval flow levels are required to satisfy the two bounds of Markovian flow levels in transmission capacity constraints as formulated in (26) and (27), so that other realizations will satisfy transmission capacity constraints

$$f_{l,g}^l(t) \geq -f_l^{\max}(t) - \sum_{i:a_l^i>0} \left[a_l^i \cdot \min_{n_i} P_{i,n_i}^M(t) \right] - \sum_{i:a_l^i<0} \left[a_l^i \cdot \max_{n_i} P_{i,n_i}^M(t) \right], \quad \forall l, \forall t, \forall g \in \{m, M\} \quad (26)$$

$$f_{l,g}^l(t) \leq f_l^{\max}(t) - \sum_{i:a_l^i>0} \left[a_l^i \cdot \max_{n_i} P_{i,n_i}^M(t) \right] - \sum_{i:a_l^i<0} \left[a_l^i \cdot \min_{n_i} P_{i,n_i}^M(t) \right], \quad \forall l, \forall t, \forall g \in \{m, M\}. \quad (27)$$

Constraints (26) and (27) are different from those in pure interval optimization (5) and (6) [18, eqs. (16) and (19)]. Pure interval optimization selects extreme combinations of wind generation (uncertain parameters), while (23) selects extreme combinations of Markovian nodal injections, which involve wind generation, the Markovian generation (decision variables), and nodal demand.

It is interesting to note that the bounds of Markovian flows in (23) are correlated with bounds of system demand, since nodal wind generation appears in both types of bounds. Thus, not all bounds will happen at the same realization, and interval generation feasible for all bounds are conservative. Nevertheless, Markovian generation in (21) can accommodate local uncertainties that appear in flows in (23), and example 1 in Section V will illustrate that the conservativeness in transmission of pure interval optimization is much alleviated.

An issue that also exists in pure interval optimization is that results are sensitive to the selection of the slack bus, and the reason will be explained in Appendix A. To alleviate this sensitivity, the distributed slack bus [31], which distributes the impacts of the slack bus into multiple buses, is adopted.

5) *Ramp Rate Constraints*: If unit_{*i,k*} is online at hours $t-1$ and t , then for all possible state transitions and the two extreme nonlocal states, the change of generation level cannot exceed the unit's ramp rate, that is

$$\begin{aligned} & p_{i,k,n_i'}^M(t-1) + p_{i,k,\bar{n}_i'}^l(t-1) - R_{i,k} \\ & \leq p_{i,k,n_i}^M(t) + p_{i,k,\bar{n}_i}^l(t) \\ & \leq p_{i,k,n_i'}^M(t-1) + p_{i,k,\bar{n}_i'}^l(t-1) + R_{i,k}, \quad \forall i, \forall k, \forall t \\ & \forall (n_i', n_i) \in \left\{ (n_i', n_i) \mid \varphi_{n_i'}(t) > 0, \pi_{n_i'} > 0 \right\} \\ & \forall \bar{n}_i \in \{m_i, M_i\}, \forall \bar{n}_i' \in \{m_i, M_i\} \end{aligned} \quad (28)$$

where \bar{n}_i' denotes the nonlocal state of node i at hour $t-1$. The changes in wind generation at possible state transitions

(except for transitions between extreme states) are smaller than those between the min and max realizations in pure interval optimization. Thus, the conservativeness in ramp rate constraints of pure interval optimization is also alleviated. In addition, generation limits at start-up and shut-down hours [32, eq. (11)] are also considered and merged with (28), based on [19, eqs. (9) and (10)].

6) *Commitment Constraints of Individual Units*:

a) *Start-up constraints*: The start-up decision is coupled with commitment decisions

$$u_{i,k}(t) \geq x_{i,k}(t) - x_{i,k}(t-1), \quad \forall i, \forall k, \forall t. \quad (29)$$

b) *Minimum up/down time*: The unit must remain online or offline for its minimum up or down time, respectively. The convex hull formulas in [33, eqs. (3) and (5)] are employed.

7) *Objective Function*: The goal of the optimization problem is to minimize the commitment cost plus the expected dispatch cost of all possible realizations rather than that of the worst-case realization to reduce conservativeness. Since the generation cost function $C_{i,k}(p_{i,k,n_i}^M(t) + p_{i,k,\bar{n}_i}^l(t))$ is piecewise linear, the cost cannot be separated into a Markovian generation cost and an interval generation cost. Given that only two extreme realizations are considered in interval generation, their costs may not reflect the costs of other possible realizations. To approximate the expected cost without much complexity, the cost of the expected realization E is included in addition to the costs of the few extreme realizations. The resulting objective function is to minimize the total weighted generation cost, plus the commitment cost, that is

$$\begin{aligned} \min & \sum_{t=1}^T \sum_{i=1}^I \sum_{k=1}^{K_i} \left\{ \sum_{n_i=1}^{N_i} [w_{n_i,m_i}(t) C_{i,k}(p_{i,k,n_i}^M(t) + p_{i,k,m_i}^l(t)) \right. \\ & \quad + w_{n_i,M_i}(t) C_{i,k}(p_{i,k,n_i}^M(t) + p_{i,k,M_i}^l(t))] \\ & \quad + w_E(t) C_{i,k}(p_{i,k,E}(t)) + u_{i,k}(t) S_{i,k} \\ & \quad \left. + x_{i,k}(t) S_{i,k}^{NL} \right\} \end{aligned} \quad (30)$$

where $w_{n_i,m_i}(t)$ is the weight of the conventional generation when local state is at n_i and nonlocal at m_i at time t , $w_{n_i,M_i}(t)$ when nonlocal at M_i , and $w_E(t)$ the expected realization. The weights among realizations are not directly selected based on corresponding probabilities. The reason is that the expected realization corresponds to no particular state and probability. Since the cost of the expected realization represents the expected cost of the vast majority of realizations, its weight should be larger than those of others. The weights $w_{n_i,m_i}(t)$ and $w_{n_i,M_i}(t)$ can further consider local probabilities. The sum of all weights at time t equals one.

The above stochastic UC problem (17)–(22), (24)–(30), and minimum up/down time constraints is a nonlinear mixed-integer optimization problem with binary decision variables $\{u_{i,k}(t)\}$ and $\{x_{i,k}(t)\}$, and continuous variables $\{p_{i,k,n_i}^M(t)\}$, $\{p_{i,k,\bar{n}_i}^l(t)\}$ and $\{p_{i,k,E}(t)\}$. The nonlinearity lies in the min/max operations of selecting extreme Markovian nodal injections in (26) and (27).

D. Discussion on Reducing the Wind Uncertainty

Two methods to reduce the wind uncertainty by considering wind power forecasts or by incorporating spatial correlations of wind farms are discussed. Testing them, however, is out of the scope of this paper.

1) *Considering Wind Power Forecasts:* With historical data only, solutions may be conservative due to the large uncertainty of day-ahead wind generation. Wind power forecasts consider weather conditions, terrain characteristics, and historical forecast errors to reduce the uncertainty [34]. Our previous work [35] converted wind power forecasts into state probabilities, instead of only using historical data based on (8), to fit in the Markovian approach. Considering wind power forecasts is expected to reduce the conservativeness of solutions.

2) *Incorporating Spatial Correlations of Wind Farms:* The outputs of nearby wind farms are likely to be correlated. Although the outputs of the wind farms are assumed to be independent for simplicity in Section III-A, incorporating the spatial correlations can help to reduce the uncertainty and thus reduce the conservativeness of solutions. A method is to aggregate the generation of nearby wind farms through aggregating buses that are connected by transmission lines with sufficient capacities. In this way, their correlations are contained in the aggregated wind generation to smooth out the uncertainty of each wind farm. An issue is to identify if transmission lines have sufficient capacities in the presence of wind uncertainty. For deterministic transmission-constrained UC problems, necessary and sufficient conditions for a transmission capacity constraint to be redundant were derived by solving an mixed-integer linear programming problem that maximizes or minimizes the flow through that line [36]. To significantly simplify the process, an analytical sufficient condition was obtained from an linear programming problem after dropping transmission constraints of other lines and integrality constraints associated with UC decisions, and were able to quickly identify most of the redundant constraints [36]. This identification method can be extended to UC with uncertain wind generation by using interval models. Buses connected by lines with sufficient capacities can then be aggregated through network reduction based on GSF matrix reduction [37], and corresponding wind generation can be aggregated. Transmission capacities of lines in the reduced network can be calculated based on QR-factorization of the reduced GSF matrix [38]. States of the aggregated wind generation will be considered with corresponding state probabilities and state transition matrices. Local and extreme nonlocal states will be based on states of aggregated wind generation at different areas.

IV. SOLUTION METHODOLOGY

The above problem is transformed into a linear form and is solved by using branch-and-cut in Section IV-A. Its complexity and conservativeness are analyzed, and are compared with those of pure Markov-based optimization and pure interval optimization in Section IV-B.

TABLE I
COMPARISON OF THE COMPLEXITY OF THE THREE APPROACHES

	No. of dispatch decisions per unit per hour	No. of flow levels per line per hour
Pure Markov-based	N'	N'
Pure Interval	2+1	2+1
Markovian and Interval	$N+2+1$	2+2+1

A. Transformation of the Min/Max Operations

To transform the min/max operations in (23), (26), and (27) into linear forms, the conjecture below describes the monotonicity of Markovian nodal injections with respect to nodal wind states. Based on this monotonicity, extreme Markovian nodal injections are selected based on indices of nodal wind states without optimization. Consider two possible local states at node i time t : state n_i and $n_i - 1$ which has less wind generation than state n_i .

1) *Monotonicity Conjecture:* The local state with lower wind generation provides less or equal to Markovian nodal injection at the optimum, that is

$$P_{i,n_i-1}^M(t) \leq P_{i,n_i}^M(t), \quad \forall i, \forall t, \forall n_i \\ \forall (n_i - 1) \in \{n_i - 1 | \varphi_{n_i-1}(t) > 0\}. \quad (31)$$

Generalized monotonicity analysis [39] will be used to support this conjecture in Appendix B. Based on the above conjecture, the minimum (maximum) Markovian nodal injection happens at the minimum (maximum) local wind generation state at the optimum, that is

$$\min_{n_i} P_{i,n_i}^M(t) = P_{i,\min n_i}^M(t), \quad \forall i, \forall t \quad (32)$$

$$\max_{n_i} P_{i,n_i}^M(t) = P_{i,\max n_i}^M(t), \quad \forall i, \forall t. \quad (33)$$

The overall problem is thus linear after including (31) as constraints and substituting the min/max operations with corresponding states of nodal injections as (32) and (33). Moreover, with state transition matrices given and state probabilities pre-computed as discussed in [19], the linearized problem can be effectively solved by using branch-and-cut.

B. Comparison of Approaches

1) *Complexity:* The complexity of the new approach is compared with those of pure Markov-based optimization and pure interval optimization in terms of the number of dispatch decisions and flow levels, because the same number of UC decisions is made. Considering I wind farms located at different buses and N states for each wind farm at each hour, Table I summarizes the comparison.

The pure Markov-based formulation is very complicated as discussed in Section III-B. The pure interval formulation is much simpler, since each unit/line at each hour has only three dispatch/flow levels corresponding to the two extreme realizations and the expected realization. Although the Markovian and interval formulation has N more dispatch decisions and two more flow levels than the pure interval formulation, the complexity is significantly reduced when compared to the pure Markov-based formulation. Furthermore, the complexity of the

new formulation does not increase as the number of distributed wind farms increases.

2) *Conservativeness*: Pure Markov-based optimization makes use of information provided by global states and state transitions. Its UC formulation is not conservative. Pure interval optimization precomputes bounds of wind uncertainty in transmission constraints without making use of local flexibility, and considers all extreme state transitions in ramp rate constraints. As a result, pure interval optimization is over conservative.

In the hybrid Markovian and interval approach, the Markovian generation makes use of information provided by local states and their transitions. The interval generation does not depend on all possible nonlocal states but extreme ones. This makes our approach more conservative than pure Markov-based optimization in transmission capacity and ramp rate constraints, and leads to more conservative UC decisions. This set of UC decisions will result in a higher simulation cost. However, our approach is still less conservative than pure interval optimization.

V. NUMERICAL RESULTS

Testing is conducted using CPLEX 12.5.1.0 [21] on a PC laptop with an Intel Core i7-2820QM 2.30 GHz CPU and 8 GB memory. Three examples of different-size problems are provided. In example 1, a simple problem is used to demonstrate that our approach is less conservative than pure interval optimization, and to illustrate dispatch decisions of our approach. In example 2, the IEEE 30-bus system is tested to demonstrate modeling accuracy and solution feasibility of our approach at different levels of wind penetration by comparing with the deterministic approach and pure interval optimization [18]. In example 3, the IEEE 118-bus system is tested to demonstrate the computational efficiency of our approach. In examples 2 and 3 where infeasibility is possible, wind curtailment and load shedding are considered. Wind curtailment is assumed to depend on local wind states for simplicity and to incur no cost. Load shedding is modeled in a manner similar to conventional generation with Markovian and interval components with a penalty of \$5000/MWh. The stopping criterion for all approaches in examples 2 and 3 is a relative mixed-integer programming gap tolerance of 0.1%.

A. Example 1

Consider a three-bus 1-h problem with two wind farms as shown in Fig. 1. This figure also shows the values and probabilities of the wind generation states, and the capacity and reactance values of the transmission lines. Table II provides the parameters of the two conventional units. For the single hour problem, time-coupling constraints such as ramp rate and minimum up/down time constraints are ignored, and the time index t is dropped.

To compare the conservativeness in transmission of the different approaches, we use the minimum transmission capacity required on the line connecting nodes 1 and 3, f_{1-3}^{\max} , to provide feasible solutions as the criterion for illustrative purposes. For pure interval optimization, the required transmission capacity

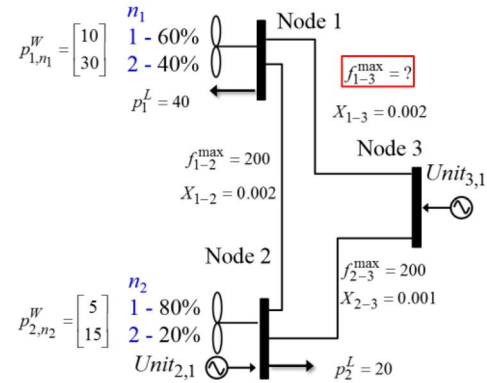


Fig. 1. Three-bus transmission network for Example 1.

TABLE II
UNIT PARAMETERS FOR EXAMPLE 1

Unit	$p_{i,k}^{\min}$ (MW)	$p_{i,k}^{\max}$ (MW)	$c_{i,k}$ (\$/MWh)
Unit _{2,1}	10	35	30
Unit _{3,1}	5	10	65

TABLE III
OPTIMIZATION RESULTS FOR EXAMPLE 1 USING THE MARKOVIAN AND INTERVAL APPROACH

Optimization cost	\$1,230.5			CPU time		0.05s
Unit	$p_{i,k,1}^M$	$p_{i,k,2}^M$	$p_{i,k,m}^I$	$p_{i,k,M}^I$	$p_{i,k}^E$	$x_{i,k}$
Unit _{2,1}	20	10	15	0	30	1
Unit _{3,1}	\	\	10	5	5	1

is 16.667 MW. For our approach, the required transmission capacity is 14 MW. Thus, our approach is less conservative in transmission.

For wind farm 1, its output p_{1,n_1}^W has two nodal states: 10 MW when $n_1 = 1$, and 30 MW when $n_1 = 2$. With another two possible nodal states at wind farm 2, there are four possible global states $[n_1, n_2]^T$: $[1, 1]^T$, $[1, 2]^T$, $[2, 1]^T$, and $[2, 2]^T$.

To illustrate the Markovian generation and interval generation of conventional units, results of our approach when $f_{1-2}^{\max} = 14$ MW are provided in Table III. Since unit_{2,1} is located at the same node as wind farm 2, its Markovian generation depends on the local state n_2 . Unit_{3,1} is not located with any local wind farm, so it does not have Markovian generation (or it equals 0). The nonlocal state of unit_{2,1} and that of unit_{3,1} are the same n_1 in this small system.

To illustrate how conventional generation realizes, simulation is conducted by fixing UC decisions at the optimal solution and solving the deterministic dispatch problem for each global state. Results are summarized in Table IV. Each unit's generation level under each global state turns out to be within the ranges delineated by sums of corresponding Markovian generation and interval generation levels.

B. Example 2

The IEEE 30-bus system is tested over a 24-h horizon with parameters adjusted as in [1]. There is a wind farm located at node 1 with a capacity of 42.5 MW. An additional wind farm

TABLE IV
SIMULATION RESULTS FOR EXAMPLE 1

$g = [n_1, n_2]^T$		$p_{2,1,g}$		$p_{3,1,g}$	
$(1, 1)^T$	$(1, 2)^T$	35	30	10	5
$(2, 1)^T$	$(2, 2)^T$	20	10	5	5

TABLE V
RESULTS FOR CASE 1 OF EXAMPLE 2

Approach		Deter.	Interval	Ours
Optimization	CPU time	2s	5s	1min4s
	Cost (k\$)	326.416	326.963	323.409
	Penalty (k\$)	0	0	0.553
UC cost (k\$)		87.642	72.616	72.201
Simulation	Cost (k\$)	360.733	325.103	323.689
	APE	9.513%	0.572%	0.087%
	STD (k\$)	56.669	15.082	14.998
	Penalty (k\$)	30.621	0	0.010

with a capacity of 28.3 MW is added to node 2. Two different levels of wind penetration are tested.

In each case, our approach is compared with the deterministic approach and pure interval optimization. For our approach, ten states are used for each wind farm based on [19], and the expected realization is calculated based on 50-state transition matrices. Based on the discussion after (30), the weights in the objective function, $w^E(t)$, $w_{n_i, m_i}(t)$, and $w_{n_i, M_i}(t)$, are set to be 0.8, $0.1\varphi_{n_i}(t)$, and $0.1\varphi_{n_i}(t)$, respectively. For pure interval optimization [18], extreme states from ten-state matrices and the expected realization from 50-state matrices are used for fair comparison. For the same purpose, the costs of the minimum and maximum realizations are also considered in the objective function, both with the same weight 0.1. The deterministic approach sets the spinning reserve levels at 3.5 STDs of hourly wind generation based on [5]. To evaluate the UC decisions obtained by different approaches, 10 000 Monte Carlo simulation runs are performed with scenarios sampled based on the 50-state transition matrices. In the simulations, UC decisions are fixed at the optimal solution, and the deterministic dispatch problem is solved repeatedly for the sampled scenarios following [7] and [11]. The simulation cost is the average cost of all sampled scenarios. Modeling accuracy of each approach is measured by the absolute percentage error (APE)

$$\text{APE} \equiv \frac{|\text{optimization cost} - \text{simulation cost}|}{\text{simulation cost}} \times 100\%. \quad (34)$$

The STD of costs of sampled scenarios reflects the variation of costs.

1) *Case 1*: State transition matrices of the two wind farms are established based on measured hourly generation data of two wind sites from April to September in 2006 (the non-winter season) from National Renewable Energy Laboratory's Eastern Wind Dataset [40], one site per wind farm. The wind penetration level, calculated as the total expected wind generation divided by the total demand without considering wind curtailment and load shedding, is 13.9%.

Results are summarized in Table V. It takes more time for our approach to reach the stopping criterion than the other two approaches. Optimization costs of the three approaches

TABLE VI
RESULTS FOR CASE 2 OF EXAMPLE 2

Approach		Deter.	Interval	Ours
Optimization	CPU time	2s	53s	1min53s
	Cost (k\$)	248.659	280.672	253.403
	Penalty (k\$)	0	0.466	0.008
UC cost (k\$)		89.461	67.715	65.216
Simulation	Cost (k\$)	314.889	263.264	250.172
	APE	21.033%	6.612%	1.292%
	STD (k\$)	74.456	33.771	35.126
	Penalty (k\$)	40.823	0	0.003

TABLE VII
RESULTS FOR EXAMPLE 3

Optimization	CPU time	49s
	Cost (k\$)	909.860
	Penalty load shedding (k\$)	0.036
	Curtailed wind (MWh)	0
UC cost (k\$)		12.690
Simulation	Cost (k\$)	907.567
	APE	0.253%
	STD (k\$)	24.188
	Penalty load shedding (k\$)	0
	Curtailed wind (MWh)	0

are very similar. However, the deterministic approach has the highest simulation cost and incurs the highest penalty cost of load shedding. This indicates that even with reserve, the deterministic approach cannot guarantee solution feasibility against all possible realizations. Both pure interval optimization and our approach are accurate in sense of their small APEs.

2) *Case 2*: To create 40% wind penetration, capacities of the two wind farms are scaled with demand unchanged. The results are summarized in Table VI. Our approach only spends about twice as much time as pure interval optimization. Our approach has a simulation cost 5.23% lower than that of pure interval optimization without incurring much penalty, indicating that our approach is less conservative. In addition, our approach is the most accurate, as it has the smallest APE.

C. Example 3

The IEEE 118-bus system [41] is tested. There are three wind farms, 54 conventional generators, 186 transmission lines, and 91 load centers with peak system demand 3733.07 MW. The wind farms use the capacities in [41], and their state transition matrices are based on measured hourly data of three wind sites from April to September in 2006 from [40]. The hourly system demand values in percent of peak system demand are calculated based on corresponding factors for summer weekdays of the IEEE Reliability Test System [42]. The wind penetration level is 7.2%. The quadratic cost curves of conventional generators are approximated by piecewise linear cost curves with three blocks.

The results of our approach are summarized in Table VII. The CPU time is 49 s, demonstrating that our approach is computational efficient. Based on the statistics provided by CPLEX, there are 150 308 constraints, 2592 binary variables, and 52 489 continuous variables (including additional decision variables for the three-block piecewise linear costs)

in optimization. The main reason why the CPU time of solving this system by using the Markovian and interval approach is even less than those in example 2 may be that the wind penetration level is lower. With relatively smaller ranges of uncertainty, it is easier to find feasible solutions.

The APE of our approach is 0.253%, demonstrating its modeling accuracy. Under this relatively low level of wind penetration, no load is shed and no wind is curtailed in any of the 10 000 simulation runs.

VI. CONCLUSION

This paper develops a synergistic combination of Markov-based optimization and interval optimization to solve the transmission-constrained UC problem with uncertain wind generation. Ideas from interval optimization are used to capture bounds of constraints to ensure solution feasibility, while Markov-based optimization uses information of local states for reduced conservativeness. Numerical results demonstrate that the new approach is effective in terms of computational efficiency, simulation cost, and solution feasibility. This paper opens a new and effective way to address stochastic problems without scenario analysis and to avoid over conservativeness. In addition, solar generation shares a similar uncertain nature as wind generation, and can thus be modeled and solved similarly.

APPENDIX A

This appendix discusses the sensitivity of results with respect to the selection of the slack bus. DC power flows can be represented by using voltage phase angles with nodal power balance constraints (that require the nodal injection to equal the sum of out flows from this node) or by using GSFs with system demand constraints (that require system-level power balance) [30]. In the deterministic approach, there is no difference between them. The reason is that when computing GSFs, one row and one column corresponding to the slack bus are taken out, assuming that system demand is satisfied. In this case, although GSF values change when the slack bus changes, power flow levels do not change. However, if the system-level power balance assumption for GSFs is not strictly satisfied as in pure interval optimization, power flow levels will change when the slack bus changes.

In pure interval optimization, on the one hand, power flow equations based on voltage phase angles cannot be used because of the following complexity. These power flow equations go hand-in-hand with nodal power balance constraints. Each nodal power balance constraint is an interval equality and will result in two constraints based on [27], similar to system demand constraints (1) and (2). When there are I nodes in a network, there will be 2^I possible combinations of these constraints to be considered at each hour. On the other hand, power flow equations with GSFs can be used to bypass this complexity, since power flows (from uncertain wind generation) can be directly substituted by a weighted sum of nodal injections. In this case, GSFs have to be computed. However, the system-level power balance assumption

for GSFs is not strictly satisfied since only bounds of system demand are considered. Consequently, when slack bus changes, GSF values change, and power flow levels change. Results are therefore sensitive to the selection of the slack bus. Results of the Markovian and interval approach have the same sensitivity issue.

APPENDIX B

This appendix is to support the monotonicity conjecture (31). Since the monotonicity is on nodal injections or dispatch decisions, we focus on the corresponding dispatch problem with UC decisions fixed. The deterministic dispatch problem, which considers a special case where the probability distribution at each hour is a singleton, will first be analyzed based on generalized monotonicity analysis [39]. When wind generation decreases, the corresponding nodal injection will decrease or remain the same. The result will then be extended to the Markovian and interval dispatch problem.

For the deterministic dispatch problem, the procedure is similar to [39, Example 4.1.2]. Lagrangian relaxation is first used to relax all constraints, namely system demand, transmission capacity, generator capacity, and ramp rate constraints. The Karush-Kuhn-Tucker (KKT) conditions [43] are used to establish a set of equalities among variables and parameters at the optimum. By taking total derivatives on both sides of the KKT conditions based on [39, eq. (2)], the directional derivative of the nodal injection will be contained in another set of equations. After solving all the above equations together, an explicit form of the directional derivative can be obtained. With the change direction of parameters imposed along the direction of wind generation, the monotonicity of the nodal injection can be observed.

Solving for this directional derivative is difficult and requires symbolic solvers. Symbolic solvers, such as Maple [44] and Symbolic Math Toolbox in MATLAB [45], do not support a general form of equations with an arbitrary size. Therefore, problems with known sizes have to be solved case by case. Moreover, the memory requirement and CPU time increase drastically as the problem size increases. Nevertheless, we solve a small case with two buses, two lines, two hours, and linear generation cost functions by using Symbolic Math Toolbox [45] in MATLAB R2013b. Due to computational limits, we first impose the change direction of parameters, v , along the direction of wind generation at node 1 at hour 2, i.e., the element in v corresponding to this wind generation, $v_{p_1}^{w(2)}$, is considered and other elements are set to zero. Then, we solve for the directional derivative of the corresponding nodal injection, $w_{p_1(2)}$, and the result is that

$$w_{p_1(2)} = v_{p_1}^{w(2)} \text{ or } 0. \quad (35)$$

This result demonstrates that the nodal injection will decrease or remain the same when wind generation decreases. The result of this small case is believed to hold in general, since all types of constraints are considered.

The above result is then extended to the Markovian and interval dispatch problem. The monotonicity can be easily applied to two deterministic cases, where the only difference

is that wind generation at node i at hour t in case 1 is less than that in case 2. Obviously, the corresponding nodal injection in case 1 will be less than or equal to that in case 2. For the pure Markov-based dispatch problem, wind generation values at states $n_i - 1$ and n_i fit into the situation of these two deterministic cases. Therefore, the nodal injection at state $n_i - 1$ will be less than or equal to that at state n_i . As for the Markovian and interval dispatch problem, since the interval nodal injection depends on extreme nonlocal states, it will not be changed by local states. Therefore, the Markovian nodal injection at state $n_i - 1$ will be less than or equal to that at state n_i .

ACKNOWLEDGMENT

The authors would like to thank the contributions of D. Schiro and I. Lelic at ISO New England, and M. Bragin at the University of Connecticut for their work on the original version of this paper.

REFERENCES

- [1] Y. Yu *et al.*, "Unit commitment with intermittent wind generation via Markovian analysis with transmission capacity constraints," in *Proc. IEEE Power Energy Soc. Gen. Meeting*, San Diego, CA, USA, Jul. 2012, pp. 1–8.
- [2] *Global Wind Report—Annual Market Update 2012*, Global Wind Energy Council, Brussels, Belgium, April 2013. [Online]. Available: http://www.gwec.net/wp-content/uploads/2012/06/Annual_report_2012_LowRes.pdf
- [3] "20% wind energy by 2030: Increasing wind energy's contribution to U.S. electricity supply," U.S. Dept. Energy, Washington, DC, USA, Tech. Rep. DOE/GO-102008-2567, Jul. 2008. [Online]. Available: <http://www.nrel.gov/docs/fy08osti/41869.pdf>
- [4] M. Holloway, "Challenges and solutions for wind integration in ERCOT," in *Proc. IEEE PES Innov. Smart Grid Technol. Conf.*, Washington, DC, USA, Mar. 2014, pp. 1–38. [Online]. Available: http://sites.ieee.org/isgt2014/files/2014/03/Day1_Panel1A_Holloway.pdf
- [5] M. Black and G. Strbac, "Value of bulk energy storage for managing wind power fluctuations," *IEEE Trans. Energy Convers.*, vol. 22, no. 1, pp. 197–205, Mar. 2007.
- [6] M. A. Ortega-Vazquez and D. S. Kirschen, "Estimating the spinning reserve requirements in systems with significant wind power generation penetration," *IEEE Trans. Power Syst.*, vol. 24, no. 1, pp. 114–124, Feb. 2009.
- [7] D. Bertsimas, E. Litvinov, X. A. Sun, J. Zhao, and T. Zheng, "Adaptive robust optimization for the security constrained unit commitment problem," *IEEE Trans. Power Syst.*, vol. 28, no. 1, pp. 52–63, Feb. 2013.
- [8] F. Bouffard and F. D. Galiana, "Stochastic security for operations planning with significant wind power generation," *IEEE Trans. Power Syst.*, vol. 23, no. 2, pp. 306–316, May 2008.
- [9] J. Wang, M. Shahidehpour, and Z. Li, "Security-constrained unit commitment with volatile wind power generation," *IEEE Trans. Power Syst.*, vol. 23, no. 3, pp. 1319–1327, Aug. 2008.
- [10] V. S. Pappala, I. Erlich, K. Rohrig, and J. Dobschinski, "A stochastic model for the optimal operation of a wind-thermal power system," *IEEE Trans. Power Syst.*, vol. 24, no. 2, pp. 940–950, May 2009.
- [11] P. Ruiz, P. C. Philbrick, E. Zak, K. W. Cheung, and P. Sauer, "Uncertainty management in the unit commitment problem," *IEEE Trans. Power Syst.*, vol. 24, no. 2, pp. 642–651, May 2009.
- [12] C. Weber, P. Meibom, R. Barth, and H. Brand, "WILMAR: A stochastic programming tool to analyze the large-scale integration of wind energy," in *Optimization in the Energy Industry*. Berlin, Germany: Springer-Verlag, 2009, ch. 19, pp. 437–458.
- [13] A. Papavasiliou, S. Oren, and R. P. O'Neill, "Reserve requirements for wind power integration: A scenario-based stochastic programming framework," *IEEE Trans. Power Syst.*, vol. 26, no. 4, pp. 2197–2206, Nov. 2011.
- [14] L. Wu, M. Shahidehpour, and Z. Li, "Comparison of scenario-based and interval optimization approaches to stochastic SCUC," *IEEE Trans. Power Syst.*, vol. 27, no. 2, pp. 913–921, May 2012.
- [15] A. Papavasiliou and S. Oren, "Multiarea stochastic unit commitment for high wind penetration in a transmission constrained network," *Oper. Res.*, vol. 61, no. 3, pp. 578–592, May/June 2013.
- [16] L. Zhao and B. Zeng, "Robust unit commitment problem with demand response and wind energy," in *Proc. IEEE Power Energy Soc. Gen. Meeting*, San Diego, CA, USA, Jul. 2012, pp. 1–8.
- [17] R. Jiang, J. Wang, and Y. Guan, "Robust unit commitment with wind power and pumped storage hydro," *IEEE Trans. Power Syst.*, vol. 27, no. 2, pp. 800–810, May 2012.
- [18] Y. Wang, Q. Xia, and C. Kang, "Unit commitment with volatile node injections by using interval optimization," *IEEE Trans. Power Syst.*, vol. 26, no. 3, pp. 1705–1713, Aug. 2011.
- [19] P. B. Luh *et al.*, "Grid integration of intermittent wind generation: A Markovian approach," *IEEE Trans. Smart Grid*, vol. 5, no. 2, pp. 732–741, Mar. 2014.
- [20] R. E. Bixby, M. Fenelon, Z. Gu, E. Rothberg, and R. Wunderling, "MIP: Theory and practice—Closing the gap," in *System Modelling and Optimization*. New York, NY, USA: Springer, 2000, pp. 19–49.
- [21] IBM ILOG. (2013). *IBM ILOG CPLEX Optimization Studio Information Center*. [Online]. Available: <http://pic.dhe.ibm.com/infocenter/cosinfoc/v12r5/index.jsp>
- [22] D. Brooks, E. Lo, R. Zavadil, S. Santoso, and J. Smith, *Characterizing the Impacts of Significant Wind Generation Facilities on Bulk Power System Operations Planning*, Xcel Energy—North Case Study, Util. Wind Interest Group, Arlington, VA, USA, May 2003. [Online]. Available: <http://www.uwig.org/UWIGOpImpactsFinal7-15-03.pdf>
- [23] NERC. (Apr. 2009). *Special Report: Accommodating High Levels of Variable Generation*. [Online]. Available: http://www.nerc.com/files/IVGTF_Report_041609.pdf
- [24] J. Dupačová, N. Gröwe-Kuska, and W. Römisch, "Scenario reduction in stochastic programming," *Math. Program.*, vol. 95, no. 3, pp. 493–511, 2003.
- [25] N. Gröwe-Kuska, H. Heitsch, and W. Römisch, "Scenario reduction and scenario tree construction for power management problems," in *Proc. 2013 IEEE Power Tech Conf.*, vol. 3. Bologna, Italy, Jun. 2003, pp. 1–7.
- [26] J. M. Morales, S. Pineda, A. J. Conejo, and M. Carrion, "Scenario reduction for futures market trading in electricity markets," *IEEE Trans. Power Syst.*, vol. 24, no. 2, pp. 878–888, May 2009.
- [27] J. W. Chinneck and K. Ramadan, "Linear programming with interval coefficients," *J. Oper. Res. Soc.*, vol. 51, no. 2, pp. 209–220, Feb. 2000.
- [28] C. Zhao and Y. Guan, "Unified stochastic and robust unit commitment," *IEEE Trans. Power Syst.*, vol. 28, no. 3, pp. 3353–3361, Aug. 2013.
- [29] Y. Dvorkin, H. Pandzic, M. A. Ortega-Vazquez, and D. S. Kirschen, "A hybrid stochastic/interval approach to transmission-constrained unit commitment," *IEEE Trans. Power Syst.*, vol. 30, no. 2, pp. 621–631, Mar. 2015.
- [30] M. Ilic, F. Galiana, and L. Fink, *Power Systems Restructuring: Engineering and Economics*. Boston, MA, USA: Kluwer Academic, 1998.
- [31] E. Litvinov, T. Zheng, G. Rosenwald, and P. Shamsollahi, "Marginal loss modeling in LMP calculation," *IEEE Trans. Power Syst.*, vol. 19, no. 2, pp. 880–888, May 2004.
- [32] X. Guan, P. B. Luh, H. Yan, and J. A. Amalfi, "An optimization-based method for unit commitment," *Int. J. Elect. Power Energy Syst.*, vol. 14, no. 1, pp. 9–17, Feb. 1992.
- [33] D. Rajan and S. Takriti, "Minimum up/down polytopes of the unit commitment problem with start-up costs," IBM T. J. Watson Res. Center, Yorktown Heights, NY, USA, Tech. Rep. RC23628, 2005.
- [34] C. Monteiro *et al.*, "Wind power forecasting: State-of-the-Art 2009," Argonne Nat. Lab., Lemont, IL, USA, Tech. Rep. ANL/DIS-10-1, Nov. 2009. [Online]. Available: <http://www.dis.anl.gov/projects/windpowerforecasting.html>
- [35] Y. Yu *et al.*, "Markov-based stochastic unit commitment considering wind power forecasts," in *Proc. IEEE Power Energy Soc. Gen. Meeting*, Vancouver, BC, Canada, Jul. 2013, pp. 1–5.
- [36] Q. Zhai, X. Guan, J. Cheng, and H. Wu, "Fast identification of inactive security constraints in SCUC problems," *IEEE Trans. Power Syst.*, vol. 25, no. 4, pp. 1946–1954, Nov. 2010.
- [37] H. Oh, "A new network reduction methodology for power system planning studies," *IEEE Trans. Power Syst.*, vol. 25, no. 2, pp. 677–684, May 2010.
- [38] H. Oh, "Aggregation of buses for a network reduction," *IEEE Trans. Power Syst.*, vol. 27, no. 2, pp. 705–712, May 2012.
- [39] B. H. Strulovici and T. A. Weber, "Generalized monotonicity analysis," *Econ. Theory*, vol. 43, no. 3, pp. 377–406, 2010.

- [40] National Renewable Energy Laboratory. (2010). *Eastern Wind Dataset*. [Online]. Available: http://www.nrel.gov/electricity/transmission/eastern_wind_methodology.html
- [41] *IEEE 118-Bus System*. (Jul. 8, 2014). [Online]. Available: <http://motor.ece.iit.edu/data/>
- [42] C. Grigg *et al.*, "The IEEE reliability test system-1996," *IEEE Trans. Power Syst.*, vol. 14, no. 3, pp. 1010–1020, Aug. 1999.
- [43] D. P. Bertsekas, *Nonlinear Programming*, 2nd ed. Belmont, MA, USA: Athena Scientific, 1999.
- [44] *Maple 18*. (Jul. 8, 2014). [Online]. Available: <http://www.maplesoft.com/products/Maple>
- [45] *Symbolic Math Toolbox*. (Jul. 8, 2014). [Online]. <http://www.mathworks.com/products/symbolic/index.html>

Yaowen Yu (S'12) received the B.S. degree in automation from the Huazhong University of Science and Technology, Wuhan, China, in 2011, and the M.S. degree in electrical engineering from the University of Connecticut, Storrs, CT, USA, in 2014. He is currently pursuing the Ph.D. degree with the University of Connecticut.

His current research interests include power system optimization, grid integration of renewable energy, and economics of electricity markets.

Peter B. Luh (S'77–M'80–SM'91–F'95) received the B.S. degree in electrical engineering from National Taiwan University, Taipei, Taiwan, in 1973; the M.S. degree in aeronautics and astronautics from the Massachusetts Institute of Technology, Cambridge, MA, USA, in 1977; and the Ph.D. degree in applied mathematics from Harvard University, Cambridge, in 1980.

He has been with the University of Connecticut, Storrs, CT, USA, since 1980, and is the SNET Professor of Communications and Information Technologies. His current research interests include smart power systems—smart grid, design of auction methods for electricity markets, effective renewable (wind and solar) integration to the grid, electricity load and price forecasting with demand response, and micro grid.

Prof. Luh was an Editor-in-Chief of the IEEE TRANSACTIONS ON ROBOTICS AND AUTOMATION, and the Founding Editor-in-Chief of the IEEE TRANSACTIONS ON AUTOMATION SCIENCE AND ENGINEERING.

Eugene Litvinov (SM'06–F'12) received the B.S. and M.S. degrees from Technical University, Kiev, Ukraine, in 1973, and the Ph.D. degree from Urals Polytechnic Institute, Sverdlovsk, Russia, in 1987.

He is currently a Chief Technologist with ISO New England, Holyoke, MA, USA. His current research interests include power system market-clearing models, system security, computer applications to power systems, and information technology.

Tongxin Zheng (SM'08) received the B.S. degree in electrical engineering from the North China Institute of Electric Power, Baoding, China, in 1993; the M.S. degree in electrical engineering from Tsinghua University, Beijing, China, in 1996; and the Ph.D. degree in electrical engineering from Clemson University, Clemson, SC, USA, in 1999.

He is currently the Technical Manager with ISO New England, Holyoke, MA, USA. His current research interests include power system optimization and electricity market design.

Jinye Zhao (M'11) received the B.S. degree from East China Normal University, Shanghai, China, in 2002; the M.S. degree in mathematics from the National University of Singapore, Singapore, in 2004; and the M.S. degree in operations research and statistics, and the Ph.D. degree in mathematics from Rensselaer Polytechnic Institute, Troy, NY, USA, in 2007.

She is currently a Lead Analyst with ISO New England, Holyoke, MA, USA. Her current research interests include game theory, mathematical programming, and electricity market modeling.

Feng Zhao (M'08) received the B.S. degree in automatic control from Shanghai Jiao Tong University, Shanghai, China, in 1998; the M.S. degree in control theory and control engineering from Tsinghua University, Beijing, China, in 2001; and the Ph.D. degree in electrical engineering from the University of Connecticut, Storrs, CT, USA, in 2008.

He is currently a Lead Analyst with ISO New England, Holyoke, MA, USA. His current research interests include mathematical optimization, power system planning and operations, and economics of electricity markets.